

# Geographic patterns and dynamics of Alaskan climate interpolated from a sparse station record

MICHAEL D. FLEMING,\* F. STUART CHAPIN III,† WOLFGANG CRAMER,‡  
GARY L. HUFFORD§ and MARK C. SERREZE¶

\*USGS/EROS Field Office, 4230 University Drive, Anchorage, AK 99508-4664, USA, †Institute of Arctic Biology, University of Alaska, Fairbanks, AK 99775, USA, ‡Potsdam Institute for Climate Impact Research, Telegrafenberg, PO Box 601203, D-14412 Potsdam, Germany, §National Weather Service, 222 W 7th Ave. Anchorage, AK 99513, USA, ¶Cooperative Institute for Research in Environmental Sciences (CIRES), Campus Box 449, University of Colorado, Boulder, CO 80309-0216, USA

## Abstract

Data from a sparse network of climate stations in Alaska were interpolated to provide 1-km resolution maps of mean monthly temperature and precipitation—variables that are required at high spatial resolution for input into regional models of ecological processes and resource management. The interpolation model is based on thin-plate smoothing splines, which uses the spatial data along with a digital elevation model to incorporate local topography. The model provides maps that are consistent with regional climatology and with patterns recognized by experienced weather forecasters. The broad patterns of Alaskan climate are well represented and include latitudinal and altitudinal trends in temperature and precipitation and gradients in continentality. Variations within these broad patterns reflect both the weakening and reduction in frequency of low-pressure centres in their eastward movement across southern Alaska during the summer, and the shift of the storm tracks into central and northern Alaska in late summer. Not surprisingly, apparent artifacts of the interpolated climate occur primarily in regions with few or no stations. The interpolation model did not accurately represent low-level winter temperature inversions that occur within large valleys and basins. Along with well-recognized climate patterns, the model captures local topographic effects that would not be depicted using standard interpolation techniques. This suggests that similar procedures could be used to generate high-resolution maps for other high-latitude regions with a sparse density of data.

*Keywords:* climate, Alaska, global change, temperature, precipitation

## Introduction

Although climate strongly affects ecological processes and human activities, climate records are only available at limited locations, usually within population centres. These stations often provide a poor representation of regional climate patterns, because they are generally biased towards coastal regions, at lower elevations along rivers and valleys, and away from mountainous and inaccessible areas. Given the biased nature of climate stations, it is challenging to estimate regional patterns of climate, particularly in sparsely inhabited high-latitude regions such as Alaska.

Two general approaches have been developed to interpolate station data for characterizing regional climate patterns. Macro-scale climatologists, who seek to describe general patterns, may not be overly concerned with physiographic biases in climate station locations, provided that simple interpolation of the available data adequately captures broad gradients associated with latitude, continentality, storm tracks and large-scale orographic effects. While simple interpolations are widely used, they often provide poor assessments of climate at any given location (see, for example, Chapman & Walsh 1993). A second, more detailed, meso-scale approach has been to incorporate patterns of complexity associated with topography, based on physical principles such as lapse rate, and use this information in conjunction with the station

Correspondence: Michael D. Fleming, tel: +1 907 786 7034, fax: 907 786 7036, e-mail: mfimages@alaska.net

data to give a continuous representation of surface climate (Running *et al.* 1987). The resulting, more detailed maps are better suited for input into models of ecological and hydrological processes and impact assessment, but are often difficult to develop and validate because of the paucity of climate stations in complex terrain.

Alaskan climate has been described in terms of synoptic patterns (Hare & Ritchie 1972; Barry & Hare 1974; Selkregg 1974; Mock *et al.* 1998). Recently, Hammond & Yarie (1996) developed maps of surface climatology, adjusted for elevation, in which they divided Alaska into 40 growing-season (May–September) climate zones and 35 annual climate zones. The present paper provides the first fine-scale maps (resolution of 1 km) of Alaskan surface temperature and precipitation, which attempt to achieve better incorporation of topographic complexity and to compensate for biases associated with station location. These maps are intended to test the feasibility of developing high-resolution climate maps for other regions of the world with sparse records. In the following, we present a brief overview of the synoptic climatology of Alaska to provide a framework for understanding the patterns that we document.

#### *Overview of Alaskan climate*

The climate of Alaska is strongly influenced by its high latitude, seasonally varying atmospheric circulation regimes and topographic effects. During winter, the primary atmospheric controls are the Aleutian Low in the Gulf of Alaska and the high frequency of anticyclonic conditions over the interior parts of the state (Moritz 1979; Serreze *et al.* 1993; Mock *et al.* 1998). Counter-clockwise circulation around the cyclones associated with the Aleutian Low advects moisture into south-eastern Alaska. Dynamical and orographic uplift combine to promote high precipitation totals and extensive cloud cover along the Gulf coast. These marine influences also result in much milder winter temperatures compared with those in the interior regions (Barry & Hare 1974; Hare & Hay 1974; Mock *et al.* 1998). The coastal mountains inhibit the flux of Pacific moisture into the interior and, coupled with the anticyclonic conditions, winter precipitation is light and cloud cover much less extensive than along the Gulf coast (Moritz 1979). Strong radiative losses caused by the limited cloud cover and the high latitude of Alaska foster low winter temperatures and the development of strong low-level inversions (Vowinckel & Orvig 1970; Hare & Hay 1974; Serreze *et al.* 1993). Because of the sea ice cover, the winter climate of the north slope of Alaska is little moderated

by the Arctic Ocean and the winter temperatures are broadly similar to those in the interior (Overland & Pease 1982).

During summer, cyclone activity associated with the Aleutian Low weakens, while anticyclonic conditions over the interior become less common. Hence, precipitation along the Gulf coast of Alaska declines from its winter maximum. However, cyclone activity tends to increase in the interior of Alaska and along the Arctic coast (Whittaker & Horn 1984), contributing to a summer precipitation peak in these areas. Some of these cyclones are associated with the Arctic front, which in July extends along the northern shores of Siberia, Alaska and eastward across northern Canada (Reed & Kunkel 1960). It is uncertain to what extent the location of the Arctic front determines the location of the treeline (Hare & Ritchie 1972), is determined by the sharp gradient in energy exchange at the boreal-tundra transition (Pielke & Vidale 1996), or is simply the result of orographic influences. Convective precipitation also contributes to the summer precipitation maximum in the interior. Summer temperatures are generally highest in the Alaskan interior, owing to seasonal heating of the land surface and distance from marine influences.

This brief overview provides a framework for interpreting the temperature and precipitation maps we present. We, of course, recognize that there are large interannual variations in Alaskan climate associated with the Arctic Oscillation (Thompson & Wallace 1998), and extratropical responses to El Niño Southern Oscillation (ENSO) forcing. For example, during moderate-to-strong ENSO warm events, above-normal temperatures are generally found over the entire state (departure from normal averaged 0.7 °C for interior, 0.4 °C for the rest of Alaska) except in the western Aleutians (–0.1 °C). There is also below-normal precipitation in the interior, Copper River Basin, the Arctic north slope and Matanuska-Susitna Valley, and above-normal precipitation along the Gulf Coast (Hess *et al.* 2000). During the 1976–77 warm episode, the coastal cities of Seward, Valdez, Cordova, Kodiak and Yakutat recorded record high precipitation between November and February, while interior Alaska experienced very dry conditions.

Interannual variations in climate provide analogues of alternative climate states that may have occurred in Alaska in the past (Mock *et al.* 1998; Edwards *et al.* in press). Recent trends in atmospheric circulation and other climate variables in Alaska suggest that high-latitude climates are changing in ways that are at least partially consistent with GCM projections of anthropogenic-induced global warming (Keyser *et al.* 2000; Serreze *et al.* 2000).

## Materials and methods

### Data sources

Historical records for stations in and around the state of Alaska were selected, and monthly climatic averages were generated for precipitation and temperature. The station averages (i.e. point samples) and a raster elevation grid were then input to a model to generate a continuous surface for each month for each variable.

The station records were obtained from the NCDC Global Historical Climatology Network (GHCN) database (Vose *et al.* 1992) that has been quality controlled with respect to both time and space. All available stations within 10 degrees of latitude or longitude of a rectangle containing the state of Alaska were selected. The average length of the station histories was about 60 years, but ranged from 10 years to 159 years. A total of 74 stations were available for temperature and 54 were available for precipitation. The location of the temperature and precipitation stations are shown in Fig. 1(a),(b), respectively. While acknowledging that the use of stations with short records could introduce biases as the record periods may not be entirely representative of climatic normals, we felt that this problem is outweighed by the need to retain as much spatial coverage as possible. The monthly GHCN records contain total precipitation and mean minimum and maximum temperature values that were used to generate long-term means. The climatological monthly means for each station are available on the project's web site. Solid precipitation is severely underestimated by standard precipitation gauges (Groisman *et al.* 1991) and, hence, the winter precipitation maps are useful primarily to assess geographical patterns of precipitation.

The interpolation model requires elevation data, both at the station locations and as a raster grid at the resolution of the final climate surfaces. The required Digital Elevation Model (DEM) data were downloaded from the US Geological Survey's EROS Data Center (EDC) Global 1-km database website at a resolution of  $15 \times 15$  arcsec. The final resolution of the surface is intended to be 1 km, so the data were resampled to a resolution of approximately 1 km over the state of Alaska,  $30 \times 60$  arcsec.

### Interpolation of climate data

Simple interpolation procedures are generally adequate to capture broad-scale influences such as latitude and continentality. However, inspection of the station data indicates that, for Alaska, as in many other areas, a major additional factor that must be addressed is the local topography, which acts in several ways:

- effects associated with elevation;
- rain-shadow effects, which result in large precipitation gradients between windward and leeward sides of major mountain chains; and;
- phenomena associated with cold air drainage, such as the development of temperature inversions in enclosed topographical settings.

Given a sufficiently dense station network, we expect that the first two effects will be reasonably well captured using an interpolation scheme explicitly addressing topography. This is because (a) the climatological lapse rate is a spatially conservative quantity, which can effectively be derived from only a few stations, and (b) the rain-shadow effect is of relevance mainly for major mountain ranges. Local cold air drainage phenomena are more difficult to address, because they strongly depend on the regional physical setting.

Previous efforts have included topographic effects in the interpolation, by applying the adiabatic lapse rate. In this approach, the lapse rate is used to reduce all station values to sea-level. The reduced data are then interpolated on a grid and the resulting grid values are scaled back to their elevation, again using the lapse rate. The argument in support of this method is that the adiabatic lapse rate provides a first-order elevation correction (Cramer & Leemans 1993). However, this approach ignores the fact that observed environmental lapse rates are rarely adiabatic and vary regionally. Moreover, the adiabatic lapse-rate technique can only be applied to temperature. Therefore, an alternative method using environmental lapse rates determined from the available observations is preferable, but it is also only applicable to temperature.

An alternative interpolation method used here, which is more suitable for sparse networks across large regions with topographical diversity, is thin-plate smoothing splines (Wahba 1979; Hutchinson 1995). The software tool ANUSPLIN (Hutchinson 1997) available from the Centre for Resources and Environmental Studies at the Australian National University, Canberra, Australia, has been tested for many areas. The fundamental advantage of this method is that it provides the option of constraining the interpolated fields not only by horizontal location (expressed by latitude and longitude), but also by vertical location (elevation). This is important, because most climate variables show strong variation with elevation. However, this variation is also often nonlinear and its rate may differ from place to place, which makes a simple scaling by altitude (such as using physically determined lapse rates) inappropriate. Here, instead, we use elevation simply as a third variable, and the resulting surfaces are defined in terms of all three spatial dimensions. We applied ANUSPLIN to each monthly set of station data, using the station coordinates

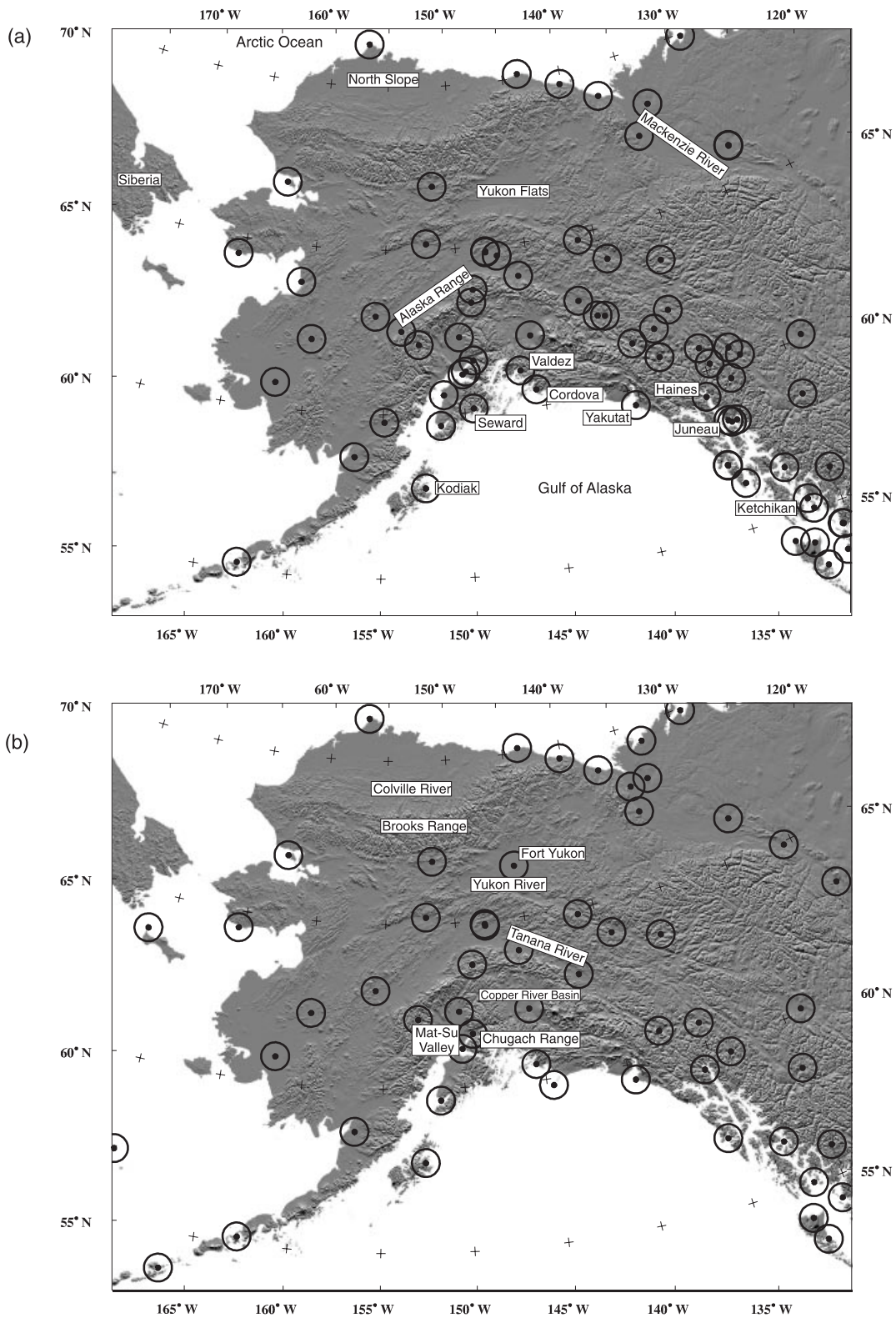


**Fig. 1** Overlay of weather station locations on a shaded-relief map: (a) temperature and (b) precipitation. These locations were used to generate the climate surface maps and represent historical records ranging from 10 to more than 150 years.

(longitude, latitude, elevation) as independent variables. This approach allows regional climate variations associated with latitude and continentality to be taken into account simultaneously with elevation and rain-shadow effects, provided that these are sufficiently captured by the station network. Therefore, the method bases the interpolation on an elevation rather than on just the adiabatic lapse rate. In fact, the lapse rates calculated from such spline surfaces will be regionally variable.

ANUSPLIN derives from the three-dimensional observations of each variable the coefficients of a spline surface. The surface is optimized using a cross-validation method, and its quality is assessed by a statistical measure of redundancy in the input data. This validation procedure assumes that there is no redundancy with respect to the description of surface features by the underlying station network, so that additional stations add new information about the pattern of each variable.

The spline surfaces can be sampled at regular intervals to provide grid-based values, given a suitable database of topography. This sampling step, which is technically separated from the derivation of the surface coefficients, must be carried out with caution, because a high-resolution grid may yield highly heterogeneous climatic patterns that cannot be validated by the sparse station data. On a relatively smooth slope, one can expect elevational boundaries to be very well represented. The climate of more complex terrain, with deep gorges or irregularly shaped peaks, is less likely to be adequately represented in the interpolation. To access potential artifacts, our resulting maps were qualitatively examined to determine whether the patterns are consistent with observations of experienced weather forecasters. We also compared the temperature and precipitation values from the climate stations that were used as model input with grid point values generated by the model. Results are discussed in the section on 'Accuracy assessment'.

### *Product generation*

The  $x$ ,  $y$ , and  $z$ (m) coordinate values from the model were assembled into a raster grid format and reprojected into an Alaska standard Albers equal-area projection with a resolution of 1 km. The raster data sets of long-term means were generated for each month for temperature (in degrees centigrade) and precipitation (in increments of 2 mm), making a total of 24 data sets. The units selected for each variable fall in the byte data range (0–255) to minimize the space requirements of the data sets.

The data sets are available through the Alaska Geospatial Data Clearinghouse website (this can be found at <http://agdc.usgs.gov>). These include the input data from the climate stations, an elevation surface grid and the output monthly climate surface grids. The

stations records are the climatic averages for each month of minimum and maximum temperature, and total precipitation. A header file is also included for each variable with the station number, station name, elevation, beginning and last year of record, latitude and longitude, and percent of missing data. The DEM data set is available at a resolution of 1 km ( $x$ ,  $y$ ) and interpolated to 1 m ( $z$ ) from 250-foot contours lines. The climate surfaces are available as grid image files that contain all 12 data sets for each variable, plus a metadata file. The precipitation images (byte) are in units of 2 mm and the mean temperature images (byte) are in units of C + 100.

## **Results and discussion**

### *Temperature*

Figure 2 shows the resulting maps for temperature for the four mid-season months of January, April, July and October. The broad geographical patterns of surface temperatures observed in and around Alaska are associated with latitude, continentality, and elevation (Fig. 2). Summer temperatures are highest (13–16 °C) in interior valleys, such as the Yukon, Tanana, and MacKenzie Rivers. The mean July temperature is 13–14 °C along the coast of south-eastern Alaska, i.e. nearly as high as in interior valleys to the north. Summer temperatures are lowest at high elevations and on the northern coastal plain, adjacent to the ice pack of the Arctic Ocean. Winter temperatures are highest (3–4 °C) in south-eastern Alaska, where the marine influence of the Gulf of Alaska is prevalent throughout the year. Interior valleys are cold in winter (–22 to –30 °C), particularly in the Mackenzie valley, which is furthest north and strongly influenced by anticyclonic conditions. As in summer, winter temperatures are lowest at high elevations.

The strongest temperature gradient is found in southern Alaska in January and near the Brooks Range in July, coinciding with the mean location of the arctic front. Other strong spatial temperature gradients are also associated with elevation, such as the relatively steep mountains of the Alaskan coastal range, the Alaska Range and the Brooks Range. There are also strong temperature gradients in south-western Alaska, associated with marine-interior gradients (SW to NE) in winter and with latitude, altitude, and direction of the prevailing wind in summer (NW to SE). On the Seward Peninsula in western Alaska, the temperature gradient switches from latitudinal (N to S) in winter to a maritime-interior (continentality) gradient (E to W) in summer, possibly as a result of the movement of the southern boundary of sea ice from south of the Seward Peninsula in winter to north of the Peninsula in summer.

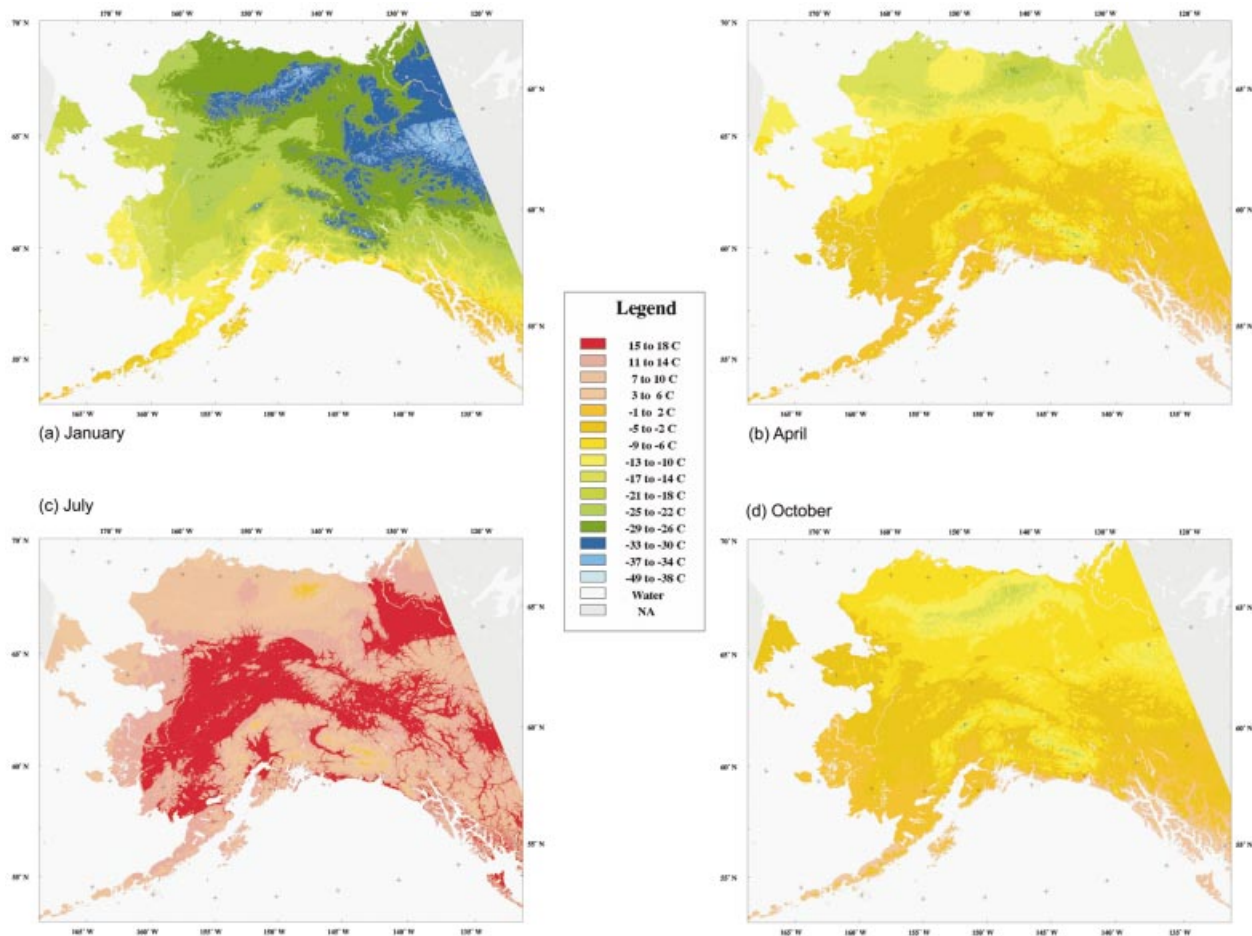


**Fig. 2** Long-term mean monthly temperature maps of Alaska generated by the model for selected months: (a) January; (b) April; (c) July; (d) October. These maps illustrate the spatial patterns of temperature across the region, aiding in interpreting and understanding of the various ecosystems.

Seasonal temperature changes are strongly driven by radiation and snow cover. Temperatures are lowest in January (Fig. 2a), except on the Arctic coast, which has a February minimum, and highest in July (Fig. 2c). Rapid warming occurs between April (Fig. 2b) and May, owing to increased solar input and the decrease in albedo associated with snowmelt. This seasonal transition is strongest in the interior, approximately 10°C, and weaker (from April to June) on the Arctic coast, reflecting later (June) snowmelt (detailed data not shown). The rapid autumn cooling coincides with reduced solar input and the return of snow cover in October (Fig. 2d).

Although most broad geographical and seasonal patterns of temperature in Alaska seem reasonable from topography and synoptic climatology, we note several anomalous patterns. In particular, there is a region of warm air over the Colville River in the central arctic coastal plain from March to August, and surprisingly high summer and low winter temperatures at 65–68°N in the Mackenzie River Valley. The warm region in the

Colville is most likely an artifact reflecting the lack of climate data. ‘Bulls-eye’ patterns are frequently produced in areas with a low density of climate stations. The summer and winter temperature extremes in Mackenzie river basin most likely reflect true climate patterns associated with the Mackenzie basin high pressure centre. The observed pattern is consistent with the four climate stations in the region.

### Precipitation

Figure 3 provides precipitation maps for the four mid-season months of January, April, July and October. As with temperature, the broad geographical patterns of precipitation estimated by the interpolation procedure are strongly associated with continentality, elevation and latitude (Fig. 3). Precipitation is highest in south-eastern Alaska and lowest on the Arctic coastal plain and interior valleys, reflecting proximity to moisture sources in the Gulf of Alaska and North Pacific. As expected,

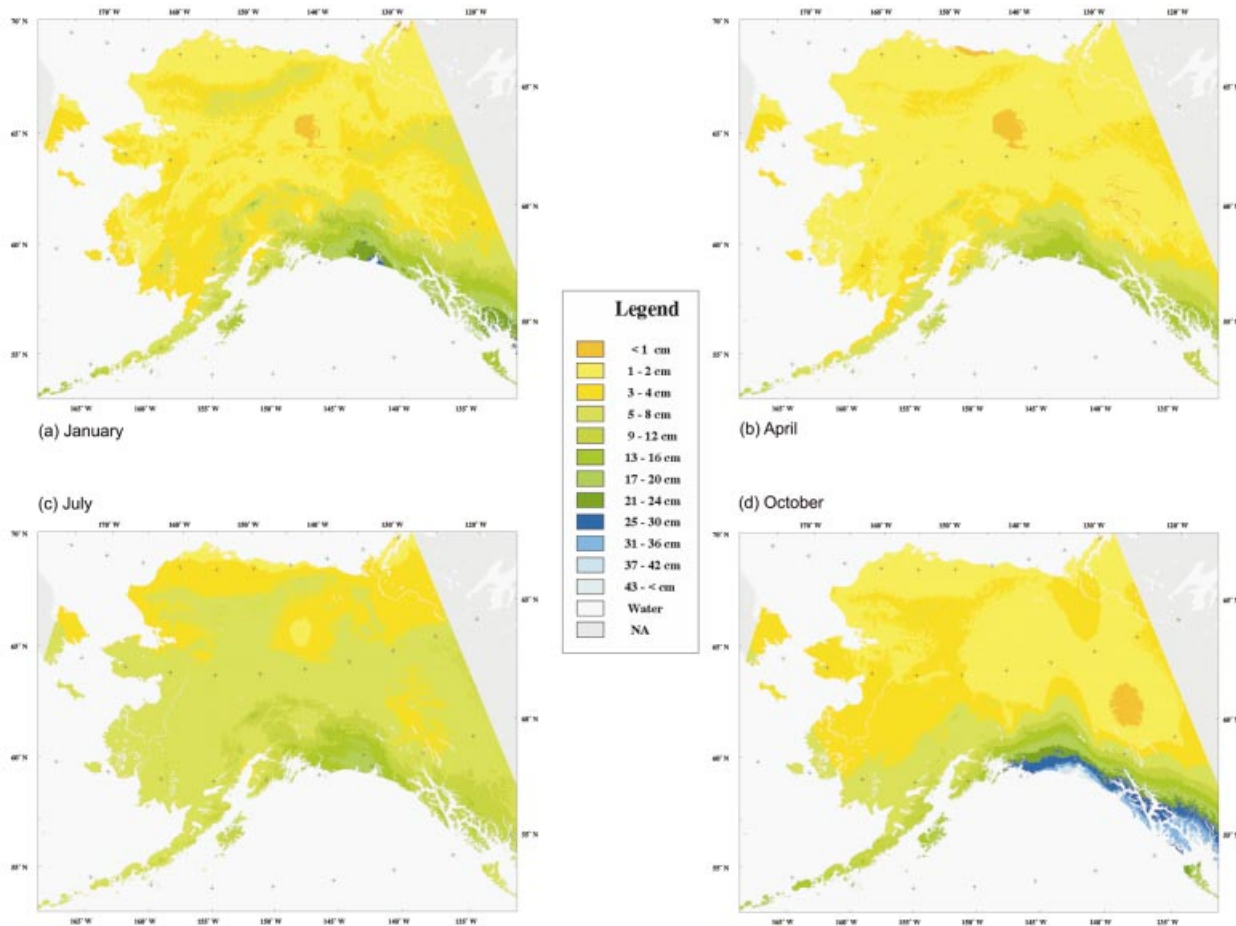


**Fig. 3** Long-term total monthly precipitation maps of Alaska generated by the model for selected months: (a) January; (b) April; (c) July; (d) October. These maps illustrate the spatial patterns of precipitation across the region, aiding in interpreting and understanding of the various ecosystems.

precipitation increases with elevation. Major rain shadows are identified by the model, such as the areas north and east of the coastal mountains, north of the Alaska Range in the Yukon flats area and areas north of the Brooks Range on the arctic coastal plain. However, the rain shadow effect is less evident in the Matanuska and Susitna valleys of south-central Alaska, and in the western end of the Chugach Mountains.

Seasonal changes in precipitation are similar to those of temperature, but lag behind temperature by 2–3 months. Thus, precipitation minima generally occur in April (Fig. 3b), with maxima in August. Surface evaporation from land provides much of the moisture for Alaskan precipitation during the summer (Walsh *et al.* 1994; Serreze *et al.* 1995). The major exception to this pattern is in south-eastern Alaska, which has its own distinct cycle that lags approximately 2 months behind the rest of the state, a June minimum and an October (Fig. 3d) maximum. This results from a weakening of the Aleutian low pressure centre in summer, and its

strengthening in autumn. The precipitation along the south-eastern coast of Alaska is the highest in the state. Even during its driest month, there is more precipitation in south-eastern Alaska than during any month in other parts of the state.

In south-eastern Alaska, the area of maximum precipitation begins increasing in July (Fig. 3c), centred near Yakutat. As the year progresses, the area of maximum precipitation expands and the centre shifts southward along the Gulf of Alaska. The highest monthly average precipitation in Alaska occurs in October, near Juneau. The centre of the area then shifts southward along the Gulf of Alaska coast and gradually decreases in size, intensity and reaches a maximum southern extent near Ketchikan in December.

Several apparent artifacts are evident in the precipitation maps. There is a strong precipitation minimum throughout the entire year in the central Yukon Valley of interior Alaska near Fort Yukon, which reflects records from the single climate station in the region. This pattern

**Table 1** Summary of statistical evaluation using historical weather station records: temperature (°C)

Month	$N^1$	Mean <sup>2</sup>	StdError <sup>3</sup>	W:Norm <sup>4</sup>	Prob < $W^5$	$t^6$	Prob > $ t ^7$
Jan <sup>+</sup>	74	0.26	0.14	0.583	0.0001	1.813	0.074
Feb	74	0.16	0.10	0.857	0.0001	1.664	0.100
Mar	74	0.13	0.10	0.859	0.0001	1.374	0.174
Apr	74	0.10	0.08	0.901	0.0001	1.235	0.221
May	74	0.05	0.07	0.930	0.0004	0.704	0.484
Jun*	74	0.13	0.06	0.958	0.0443	2.112	0.038
Jul	74	0.07	0.06	0.972	0.2888	1.278	0.205
Aug	74	0.06	0.06	0.926	0.0002	1.057	0.294
Sep	74	0.11	0.07	0.890	0.0001	1.616	0.111
Oct*	74	0.14	0.07	0.835	0.0001	2.133	0.036
Nov	74	0.11	0.08	0.805	0.0001	1.291	0.201
Dec <sup>+</sup>	74	0.17	0.09	0.852	0.0001	1.830	0.071

<sup>1</sup> $N$ , sample size (number of historical station records). <sup>2</sup>Mean, mean of the difference between the model predictions and actual long-term means. <sup>3</sup>StdError, standard error of the mean difference. <sup>4</sup>W:Norm, Shapiro–Wilk statistic, test for normality of the difference distribution. <sup>5</sup>Prob <  $W$ , probability of Shapiro–Wilk statistic. <sup>6</sup> $t$ ,  $t$  statistic to estimate the probability that the mean difference is zero. <sup>7</sup>Prob >  $|t|$ , probability that the mean difference is zero. <sup>+</sup> $t$  significant at 0.10, \* $t$  significant at 0.05.

is most obvious in months when precipitation falls as snow (October–April). Standard precipitation gauges are notorious for underestimating snowfall, often by as much as 50–75% (Groisman *et al.* 1991), suggesting that the anomalous pattern may reflect both poor-quality data and a paucity of climate stations. Note the precipitation maximum in October and minimum in June–August in the Mackenzie River. While contrasting with other continental areas, this seasonality is observed in all the Mackenzie basin climate stations, so is a real feature.

#### Accuracy assessment

Our map patterns are generally consistent with the Alaskan climate zones of Hammond & Yarie (1996), with coarse-scale isopleths of temperature and precipitation for the state (Selkregg 1974), and with climate maps for subregions such as the North Slope of Alaska (Moritz 1979; Thoman 1990), interior Alaska (Santeford 1976; Bowling 1977), and a north–south transect from the Arctic to the Pacific Ocean along the Alaska pipeline (Searby 1968).

The historical station records were used to evaluate results from the continuous surface model. There were other stations that are not part of the original data set, but these stations generally have shorter records and have not been quality checked. Thus, the evaluation is biased towards the more populated areas along rivers and the coast, and the accuracy of the model is expected to be higher in these areas. The evaluation consisted of comparing the long-term station averages and values generated by the model. A paired comparison  $t$ -test was used to test the assumption that the distribution of the

differences between the observed and the model values had a mean equal to zero (i.e. no difference) and was normally distributed.

The error analysis was performed for each month for both variables. Results summarized in Tables 1 (temperature) and 2 (precipitation) indicate that, in general, the null hypothesis cannot be rejected, i.e. mean difference between the model and the observed data is zero. There is a significant difference between modelled and observed temperature for two months (June and October;  $P < 0.05$ ) and a marginally significant difference in two additional months (January and December;  $P < 0.1$ ). The differences between modelled and observed temperature average less than 0.2 °C in all months. There are no significant differences between modelled and observed precipitation.

One assumption of the Student's  $t$ -statistic is that the differences are normally distributed. The Shapiro–Wilk (W:Norm) test for normality was used to test the distributions and is included with probability values (Prob <  $W$ ) in Tables 1 and 2. Evaluation of the Shapiro–Wilk statistic indicates that, for most months and for both precipitation and temperature, the differences are not normally distributed. Analysis of the differences indicates that, for both variables, the distribution is symmetrical around zero, but has quite a large spike at zero and a few outliers. The large number of differences of zero or less than 1 °C indicates that, at the input stations, the surfaces fit the data. There are also a small number of outlier stations with relatively large differences. After dropping these stations, the Shapiro–Wilk values increased enough that almost all months passed the normality test for both variables.

**Table 2** Summary of statistical evaluation using historical weather station records: precipitation (mm)

Month	N <sup>1</sup>	Mean <sup>2</sup>	StdError <sup>3</sup>	W:Norm <sup>4</sup>	Prob < W <sup>5</sup>	t <sup>6</sup>	Prob >  t  <sup>7</sup>
Jan	54	-0.24	0.68	0.682	0.0001	-0.344	0.732
Feb	54	-0.07	0.48	0.804	0.0001	-0.136	0.893
Mar	54	-0.25	0.53	0.787	0.0001	-0.474	0.638
Apr	54	-0.09	0.44	0.769	0.0001	-0.195	0.846
May	54	-0.18	0.48	0.711	0.0001	-0.378	0.707
Jun	54	-0.69	0.55	0.798	0.0001	-1.256	0.215
Jul	54	-0.44	0.56	0.797	0.0001	-0.775	0.442
Aug	54	-0.43	0.62	0.674	0.0001	-0.701	0.487
Sep	54	0.19	0.62	0.914	0.0006	0.298	0.767
Oct	54	0.80	0.68	0.872	0.0001	1.177	0.245
Nov	54	0.05	0.57	0.821	0.0001	0.091	0.928
Dec	54	-0.38	0.72	0.734	0.0001	-0.519	0.606

<sup>1</sup>N, sample size (number of historical station records). <sup>2</sup>Mean, mean of the difference between the model predictions and actual long-term means. <sup>3</sup>StdError, standard error of the mean difference. <sup>4</sup>W:Norm, Shapiro–Wilk statistic, test for normality of the difference distribution. <sup>5</sup>Prob < W, probability of Shapiro–Wilk statistic. <sup>6</sup>t, t statistic to estimate the probability that the mean difference is zero. <sup>7</sup>Prob > |t|, probability that the mean difference is zero.

Overall, the modelled values fit the station values quite well. The average difference for all months of precipitation is 0.3 mm with a standard error of 0.6, and modelled temperature differs from observations by 0.12 °C with a standard error of 0.08. The precipitation model has a tendency to overestimate the values, except in three months (September–November) when the model underestimates precipitation. Temperatures are consistently underestimated, particularly in winter.

Analysis of the distribution of stations for which values are poorly predicted by the model show several interesting patterns. All the outlying stations for the temperature are located along the coastline of the Gulf of Alaska (Seward, Valdez, Haines and Premier, BC). The monthly temperatures at these four stations are consistently underestimated, with the worst estimates occurring during the winter months. The two outlying stations for precipitation data are both located in the middle of the Alaska Range, McKinley Park and Puntilla. For these stations, the model consistently overestimates monthly precipitation. The discrepancy could reflect problems in the way elevation is treated. The two stations with largest discrepancies are higher in altitude and are surrounded by stations at lower elevations. These two stations may be influenced by local rain shadow effects.

The maps generated were also given to the lead weather forecasters at the National Weather Service Forecast Offices in Juneau, Anchorage and Fairbanks, for their review. The forecasters generally agreed with the temperature and precipitation patterns, except for issues already raised in this paper: lack of temperature inversions in the valleys, especially in the interior; and lack of rain shadows in a few areas. All the

forecasters agreed that they would use the maps to train junior forecasters on weather patterns across Alaska.

## Conclusions

Our study demonstrates that reasonable climatic maps can be generated at a resolution of 1 km, even in regions with a low density of climate stations. These maps are at the same spatial scale as the AVHRR (advanced very high resolution radiometer) satellite data and the derived NDVI (normalized difference vegetation index) data, which are available for the entire globe. In Alaska, maps at a resolution of 1 km are also available for elevation, vegetation, permafrost and soils. Taken together, these provided spatially explicit data for most of the input variables required for ecological modelling (ADGC 1998). Since most regional management decisions require information at a relatively fine scale, the development of 1-km climate maps will have applications for assessing potential impacts of climatic change. To this end, a next step is to develop grid-based time series of climate records. This has been accomplished by VEMAP for the contiguous United States (Kittel *et al.* 1996) and is currently being addressed for Alaska.

## Acknowledgements

This research was stimulated by a workshop organized by the US National Center for Ecological Analysis and Synthesis, and was supported by NSF grants for Arctic System Science (Grants OPP-9523396, OPP-9732461, OPP-9906906), the Long-Term Ecological Research (Grant DEB-9211769), by NASA (Grant TE/97-0032) and the USGS/EROS Alaska Field Office.

## References

- Barry RG, Hare FK (1974) Arctic climate. In: *Arctic and Alpine Environments* (eds Ives JD, Barry RG), pp. 17–54. Methuen, London.
- Bowling SA (1977) Relationships between temperature and snowfall in interior Alaska. *Arctic*, **30**, 62–64.
- Chapman WL, Walsh JE (1993) Recent variations of sea ice and air temperature in high latitudes. *Bulletin of the American Meteorological Society*, **74**, 33–47.
- Cramer W, Leemans R (1993) Assessing impacts of climate change on vegetation using climate classification systems. In: *Vegetation Dynamics and Global Change* (eds Solomon AM, Shugart HH), pp. 190–217. Chapman & Hall, New York.
- Edwards ME, Mock CJ, Finney BP, Barber VA, Bartlein PJ (2000) Modern-climate analogues for paleoclimatic variations in eastern interior Alaska during the past 14,000 years: atmospheric-circulation controls of regional temperature and moisture responses. *Quaternary Science Reviews*, in press.
- Groisman PY, Koknaeva VV, Belokrylova TA, Karl TR (1991) Overcoming biases of precipitation: a history of the USSR experience. *Bulletin of the American Meteorological Society*, **72**, 1725–1733.
- Hammond T, Yarie J (1996) Spatial prediction of climate state factor regions in Alaska. *Ecoscience*, **3**, 490–501.
- Hare FK, Hay JE (1974) The climate of Canada and Alaska, Chapter 2. In: *World Survey of Climatology*, Vol. 11, *Climates of North America* (eds Bryson RA, Hare FK), pp. 48–192. Elsevier, Amsterdam.
- Hare FK, Ritchie JC (1972) The boreal bioclimates. *Geographical Review*, **62**, 333–365.
- Hess J, Scott JC, Hufford G, Fleming MD (2000) El Niño and its impact on fire weather conditions in Alaska. *International Journal of Wildland Fire*, in press.
- Hutchinson MF (1995) Interpolating mean rainfall using thin plate smoothing splines. *International Journal for Geographical Information Systems*, **9**, 385–403.
- Hutchinson MF (1997) ANUSPLIN, Version 3.2, <http://cres.anu.edu.au/software/anusplin.html>.
- Keyser AR, Kimball JS, Nemani RR, Running SW (2000) Simulating the effects of climatic change on the carbon balance of North American high-latitude forests. *Global Change Biology*, in press.
- Kittel TGF, Rosenbloom NA, Painter TH, Schimel DS, Fisher HH, Grimsdell A, Daly C, Hunt ER Jr (1996) *The VEMAP Phase I Database: An Integrated Input Dataset for Ecosystem and Vegetation Modeling for the Conterminous United States*. CD-ROM and web site: <http://www.cgd.ucar.edu/vemap/>.
- Mock CJ, Bartlein PJ, Anderson PM (1998) Atmospheric circulation patterns and spatial climate variations in Beringia. *International Journal of Climatology*, **10**, 1085–1104.
- Moritz RE (1979) *Synoptic climatology of the Beaufort Sea coast of Alaska*. Institute of Arctic and Alpine Research, University of Colorado.
- Overland JE, Pease CH (1982) Cyclone climatology of the Bering Sea and its relation to sea ice extent. *Monthly Weather Review*, **110**, 5–13.
- Pielke RA, Vidale PL (1996) The boreal forest and the polar front. *Journal of Geophysical Research-Atmospheres*, **100D**, 25755–25758.
- Reed RJ, Kunkel BA (1960) The Arctic circulation in summer. *Journal of Meteorology*, **17**, 489–505.
- Running SW, Nemani RR, Hungerford RD (1987) Extrapolation of synoptic meteorological data in mountainous terrain and its use for simulating forest evapotranspiration and photosynthesis. *Canadian Journal of Forest Research*, **17**, 474–483.
- Santeford HS (1976) A preliminary analysis of precipitation in the Chena Basin. *NOAA Technical Memorandum NWS AR-15*. US Department of Commerce, National Oceanic and Atmospheric Administration, Anchorage, AK.
- Searby HW (1968) Climate along a pipeline from the Arctic to the Gulf of Alaska. *NOAA Technical Memorandum NWS AR-02*. US Department of Commerce, National Oceanic and Atmospheric Administration, Anchorage, AK.
- Selkregg LL (1974) *Alaska Regional Profiles*. University of Alaska Arctic Information and Data Center, Anchorage, AK.
- Serreze MC, Box JE, Barry RG, Walsh JE (1993) Characteristics of Arctic synoptic activity. 1952–89, *Meteorology and Atmospheric Physics*, 147–164.
- Serreze MC, Barry RG, Walsh JE (1995) Atmospheric water vapor characteristics at 70°N. *Journal of Climate*, **8**, 719–731.
- Serreze MC, Walsh JE, Chapin FS III, Osterkamp T, Dyrgerov M, Romanovsky V, Oechel WC, Morison J, Zhang T, Barry RG (2000) Observational evidence of recent change in the northern high-latitude environment. *Climatic Change*, in press.
- Thoman RL (1990) The climate of Prudhoe Bay, Alaska. *NOAA Technical Memorandum NWS AR-44*. US Department of Commerce, National Oceanic and Atmospheric Administration, Anchorage, AK.
- Thompson DJW, Wallace JM (1998) The Arctic Oscillation signature in the wintertime geopotential height and temperature fields. *Geophysical Research Letters*, **25**, 1297–1300.
- Vose RS, Schroyer RL, Steurer PM, Peterson TC, Heim R, Karl TR, Eischeid J (1992) The Global Historical Climatology Network: Long-term monthly temperature, precipitation, sea level pressure, and station pressure data. *ORNL/CDIAC-53, NDP-041*. Carbon Dioxide Information Analysis Center, Oak Ridge National Laboratory, Oak Ridge, TN.
- Vowinckel E, Orvig S (1970) The climate of the North Polar Basin. In: *World Survey of Climatology*, Vol. 14, *Climates of the Polar Regions* (ed. Orvig S), pp. 129–252. Elsevier, Amsterdam.
- Wahba G (1979) How to smooth curves and surfaces with splines and cross-validation. In: *24th Design of Experiments Conference, Madison, WI, 3–5 May 1978*, pp. 167–192. US Army Research Office, Research Triangle Park, NC.
- Walsh JE, Zhou X, Portis D, Serreze M (1994) Atmospheric contribution to hydrologic variations in the arctic. *Atmosphere-Ocean*, **32**, 733–755.
- Whittaker LM, Horn LH (1984) Northern Hemisphere extratropical cyclone activity for four mid-season months. *Journal of Climatology*, **4**, 297–310.